FERMI ACCELERATION REVISITED

by

A. J. Lichtenberg, M. A. Lieberman and R. H. Cohen

Memorandum No. UCB/ERL M80/36

1 September 1980

ELECTRONICS RESEARCH LABORATORY

College of Engineering
University of California, Berkeley
94720

FERMI ACCELERATION REVISITED

by

A. J. Lichtenberg and M. A. Lieberman, University of California, Berkeley CA 94720, and R. H. Cohen, Lawrence Livermore Laboratory, Livermore CA 94550.

ABSTRACT

Mappings that have been used to describe the Fermi acceleration mechanism are examined. It is shown that results which appear to be contradictory are due to differences in the mapping equations. For those mappings that can be locally approximated by the standard mapping, the value of the nonlinear parameter of the standard mapping, for which the last isolating KAM surface exists, can be used to predict the loss of KAM stability with action for the more general mappings. Previous results of the variation in the density distribution in the stochastic region of the phase space, averaged over phases, is shown to be consistent with the ergodic hypothesis. Fine scale structure of the mappings is found to be model dependent. The standard mapping is a member of a class of mappings which retains some KAM trajectories at arbitrarily large nonlinearity. This feature is not generic to a wider class of mappings discussed in this paper. The stability of two-iteration fixed points are discussed in detail, including the bifurcation sequence for one type of mapping.

FERMI ACCELERATION REVISITED

by

A. J. Lichtenberg and M. A. Lieberman, University of California, Berkeley CA 94720, and R. H. Cohen, Lawrence Livermore Laboratory, Livermore CA 94550.

I. INTRODUCTION

As an explanation for the origin of cosmic rays, Fermi [1] proposed a mechanism for charged particles to accelerate by collisions with moving magnetic field structures. The process is analogous to elastic collisions between a light and heavy object, and a simple version, that of a light particle bouncing between a fixed and an oscillating wall, was first examined by Ulam and associates [2]. If the phase of the wall oscillation is chosen randomly at the time of impact, then the obvious result is obtained, that the particle is accelerated on the average, as found by Hammersley [3]. The more interesting theoretical question is whether stochastic acceleration can result from the nonlinear dynamics alone, in the absence of an imposed random phase assumption, i.e., when the wall oscillation is a periodic function of time. Numerical simulations of this case, reported by Ulam [2] indicated that the particle motion appeared to be stochastic, but did not increase its energy on the average.

Ulam's result was explained by a combination of analytic and numerical work by Zaslavskii and Chirikov [4] and, more completely, by Brahic [5] and by Lieberman and Lichtenberg [6]. They showed that the phase space was divided into three regions: (1) low velocities for

which the phase space is essentially stochastic; (II) intermediate velocities for which islands of regular motion are imbedded in the stochastic sea; and (III) high velocities for which most trajectories are regular and bounded. Furthermore, if the periodic wall velocity has a sufficient number of continuous derivatives, invariant curves span the phase space, separating the stochastic sea of regions I and II, from region III, and thus bound the energy gain of the particles. This last result is in agreement with the Kolmogorov-Arnold-Moser (KAM) theorem, which states that for dynamical systems sufficiently close to integrable ones most regular surfaces characteristic of integral systems continue to exist (see, for example, Arnold [7]). The lowest value of velocity at which a KAM surface isolates higher velocities from stochastic motion at lower velocities can not be determined from the rigorous theory. This transition has been found numerically and compared with more heuristic theories (see Lieberman and Lichtenberg [6]).

Because the Fermi particle acceleration mechanism was: (a) one of the first considered for determining the regions of parameter space where KAM surfaces existed, (b) easily approximated by simple mappings for which numerical solutions are attainable for "long times", and (c) has the important physical application of cosmic ray production, it has become a bellweather problem in understanding the dynamics of nonlinear Hamiltonian systems with the equivalent of two degrees of freedom. Consequently, it is important to understand which features of the problem are generic to near-integrable systems and which are model-dependent. This is of particular importance in that various models of Fermi acceleration, and their approximations, have produced results that, at least superficially, appear to be contradictory.

There have been several important models considered in the literature, each described by a different surface of section mapping. The Ulam configuration of a particle bouncing between a fixed and an oscillating wall is illustrated in Fig. 1a, and has been treated using an "exact" dynamical mapping for a sawtooth wall velocity by Zaslavskii and Chirikov [4], and Lieberman and Lichtenberg [6], and with both sawtooth and parabolic wall velocties by Brahic [5]. A "simplified" Ulam mapping, in which the oscillating wall imparts momentum to the particle but occupies a fixed position, was introduced by Lieberman and Lichtenberg [6] and studied for arbitrary wall velocity. This simplified version approximates many (but not all) features of the exact mapping, provided the particle velocity is much larger than the wall velocity.

Pustylnikov [8] has considered a different configuration, illustrated in Fig. 1b, in which the particle strikes a single oscillating wall and returns to it under the influence of a constant gravitational force. He treats this problem using an exact dynamical mapping for arbitrary wall velocities. Again, a simplified mapping may be introduced, which approximates the oscillating wall interaction by one that imparts momentum at a fixed position.

Pustylnikov showed rigorously, using the exact form of his mapping, that, even for analytic wall velocities, parameters can be chosen such that there is no bound to the energy gain of the particle; i.e., "globally isolating" KAM surfaces do not exist, differing from results on the Ulam model, which exhibited KAM surfaces bounding the energy increase. In Section II, we show that Pustylnikov's result arises from the nature of his mapping, and that no contradiction to previous results exists.

In Section III, an apparent disagreement in the diffusion within the primary stochastic sea, between the exact and simplified Ulam mappings, is resolved. The resolution was first pointed out by Izrailev and Zhdanova [16] for the case of a sawtooth wall velocity. Their calculation is extended to arbitrary wall velocity in Section III.

When studying the motion in the neighborhood of a given energy, it is often possible to linearize about a given value of the action to obtain a "standard mapping" (see Chirikov [9]). For the standard mapping two-iteration stable periodic points are known to persist for arbitrarily large values of the nonlinearity parameter [9], corresponding to arbitrarily small values of the particle energy for the Ulam mapping which locally approximates it. This is in distinction to the results in Lieberman and Lichtenberg [6], who found a lower energy bound on the stability of these periodic points. This difference is explained in Sec. IV where it is shown that a fundamental difference exists between a class of mappings including the Ulam version of Fermi acceleration, and a class of mappings which includes the approximation of the standard mapping, resulting in the contrasting stability conditions at two-iteration points.

II. EXISTENCE OF ISOLATING KAM SURFACES

In the version of the Fermi acceleration problem, treated in a rigorous mathematical way by Pustylnikov [8], the particle strikes a single oscillating wall and returns to it under the action of a constant gravitational force. The problem is similar to that formulated by Ulam, in which the particle returns to the oscillating wall by reflection from a fixed wall in that it is a one degree of freedom non-autonomous Hamil-

tonian system that can be represented by an area preserving mapping. However, in contrast to Ulam's configuration, Pustylnikov finds that, even for an analytic wall velocity, there exist conditions for which a finite measure of the initial conditions will result in an unbounded increase in the particle velocity. He concludes that this result is "in agreement" with unbounded velocities found by Zaslavskii [10] for a sawtooth wall velocity in Ulam's configuration, and is a counter example to the statement of Zaslavskii and Chirikov [4] that the stochastic motion will be ergodic, i.e., uniformly fill the available phase space. These conclusions, with a rigorous mathematical calculation to back them up, appear at first glance to throw into doubt the more heuristic techniques (see, for example, Chirikov [9]) that have been developed to calculate the behavior of these systems.

We now demonstrate that there is no contradiction between the implications of Pustylnikov's [8] results for the gravitational return problem and those for the fixed wall reflective return problem, for analytic wall velocities. Furthermore, the lack of a KAM barrier with a sawtooth wall velocity arises from a different effect than that in the Pustylnikov calculation. We show that with a smooth wall oscillation, for the Ulam configuration, a particle bouncing between a fixed and oscillating wall is bounded in velocity, while, for the Pustylnikov configuration, a particle returning to an oscillatory wall due to gravity may have unbounded motion. The nature of this difference lies in the physical difference between the two problems. The transit time between wall collisions decreases with increasing particle velocity for the Ulam configuration and increases with increasing velocity for the Pustylnikov configuration.

We consider a wall motion $x_w = aF(\phi)$, where F is an even periodic function of the phase $\phi = \omega t$, period 2π , with $F_{max} = -F_{min} = 1$. For convenience, we consider the simplified Ulam and Pustylnikov mappings, in which the moving wall imparts momentum to the particle but occupies a fixed position, such that the transit time between successive collisions is independent of the phase of the moving wall. Then the motion of the particle in either configuration is given by the difference equations

$$u_{n+1} = u_n - F'(\phi_n) \tag{1}$$

$$\phi_{n+1} = \phi_n + \omega\tau(u_{n+1}) \tag{2}$$

where $\phi_n = \omega t_n$ is the wall oscillation phase just before the n^{th} collision with the moving wall, $u_n = v_n/2\omega a$ is the normalized particle velocity, τ is the time between the n^{th} and $(n+1)^{st}$ collision, and F' is the derivative of F with respect to ϕ and represents the velocity impulse given to the particle. Equations (1) and (2) consist of two shears, that is, two mappings in which one variable is advanced with the other fixed, and are area preserving. Furthermore, for F' sufficiently smooth and for F'/u sufficiently small, KAM curves exist (e.g., see Moser [11]). With $F' \equiv 0$, these equations describe integrable motion on a torus $u = \text{const}$, with the phase advancing in equal increments.

For the simplified Ulam mapping,

$$\tau = 2\ell/v_{n+1} \tag{3}$$

where ℓ is the distance between the walls. For determination of KAM surfaces we are interested in values of $u \gg F'$. In this limit, ϕ changes much more rapidly than v so that we can examine a localized region of the

phase space in the neighborhood of some v_o satisfying

$$\omega\tau(v_o) = 2\pi m \quad , \quad m \text{ integer} \ , \tag{4}$$

which is the value of v_o for stationary phase (modulo 2π). We expand τ as

$$\omega\tau(v_{n+1}) = 2\pi m + \omega \left.\frac{d\tau}{dv}\right|_{v_{n+1}} \Delta v_{n+1} \tag{5}$$

where τ is given in (3). Furthermore, we take $F = \cos\phi$, which is analytic and therefore satisfies the KAM smoothness criterion. With these substitutions (1) and (2) become

$$\Delta u_{n+1} = \Delta u_n + \sin \Delta\phi_n \tag{6}$$

$$\Delta\phi_{n+1} = \Delta\phi_n - \frac{2\omega^2 a\ell}{v_o^2} \Delta u_{n+1} \tag{7}$$

where $\Delta\phi_n = \phi_n - \phi_{on}$ and $\phi_{on+1} = \phi_{on} + 2\pi m$.

This mapping can be compared with that obtained from Pustylnikov's problem. There we set

$$\tau = 2v_{n+1}/g \tag{8}$$

which when substituted in (2), with $F' = -\sin\phi_n$, as above, gives the mapping

$$u_{n+1} = u_n + \sin \phi_n \tag{9}$$

$$\phi_{n+1} = \phi_n + \frac{4\omega^2 a}{g} u_{n+1} \ . \tag{10}$$

The mappings in (6)-(7) and (9)-(10) have the same form, valid for a localized region in velocity in the former case. However, a fundamental difference is that the coefficient of u_{n+1} is independent of velocity in (10) while in (7) it is inversely dependent on v_o. The physical consequence is that the change in ϕ due to a change in v continues to have the same proportionality, independent of v, in the case of (10); while for (7) this proportionality factor becomes increasingly small with increasing v. Since it is the phase randomization resulting from this term that we would expect to be the source of the stochasiticty, we would therefore also expect stochasticity to be limited with increasing energy in the case of the mapping in (6)-(7), but not in the case of the mapping in (9)-(10). We can see this formally by introducing the changes in variables

$$I = \begin{cases} -\dfrac{2\omega^2 a\ell}{v_o^2}\,\Delta u \quad , & \text{in (6)} \\ \dfrac{4\omega^2 a}{g}\,u \quad , & \text{in (9)} \end{cases}$$

$$\theta = \begin{cases} \Delta\phi \quad , & \text{in (7)} \\ \phi \quad , & \text{in (10)} \end{cases} \qquad (11)$$

obtaining for both equations a form known as the standard mapping.

$$I_{n+1} = I_n + \bar{K}\cos\theta \qquad (12)$$

$$\theta_{n+1} = \theta_n + I_{n+1} \quad . \qquad (13)$$

We emphasize that the mapping of (12) and (13) approximates that of (6) and (7), only locally, while it is globally equivalent to (9) and (10). A wide variety of other mappings have also been approximated by the standard mapping over a limited portion of the action space, such as the separatrix mapping of the pendulum (e.g., Chirikov [9]) and the motion of particles in mirror machines (e.g., Chirikov [9], and Cohen [12]). The standard mapping is periodic (period 2π) in both I and θ . It has been extensively studied by a combination of analytic and numerical techniques (see Chirikov [9], Greene [13], and Lichtenberg [14]), indicating the existence of a KAM surface, "globally" isolating regions of I, separated by 2π intervals for $\bar{K} \lesssim 1$. (Green [13] obtains the most precise result of $K \leq 0.97$.) For the mapping of (6)-(7) this implies that a globally isolating KAM surface exists for

$$v_o < 0.97\, \omega(2a\ell)^{\frac{1}{2}} . \tag{14}$$

For the mapping of (9)-(10) this implies that no globally isolating KAM surface exists for any v , provided

$$\frac{4\omega^2 a}{g} > 0.97 \tag{15}$$

This calculation interprets the mathematical result of Pustylnikov, and resolves the apparent contradiction raised by him. Numerical calculations have been performed by Lieberman and Lichtenberg [6], for the problem of the ball contained between the fixed and oscillating walls. They found that the position of the isolating KAM surface is in excellent agreement with the prediction of the standard mapping approximation given by (14).

We now discuss, briefly, the reason for the unbounded velocity observed by Zaslavskii [10] and also by Lieberman and Lichtenberg [6], for the sawtooth wall velocity, in the Ulam version of Fermi acceleration. The sawtooth forcing function is discontinuous at its edges and consequently does not satisfy the KAM theorem which requires some number of continuous derivatives of the function. Moser [11] estimated that three continuous derivatives of F were sufficient for the existence of KAM surfaces. In Lieberman and Lichtenberg, Figs. 2 and 3, the trajectories of particles, were computed obeying the sawtooth velocity function

$$F' = \{\phi_n\} - \frac{1}{2} \quad , \tag{16}$$

and the cubic forcing function

$$F' = (2\{\phi_n\} - 1)[1 - (2\{\phi_n\}-1)^2] \quad , \tag{17}$$

where $\{\phi_n\}$ is the fractional part of ϕ_n .
For the latter, F'' is continuous and F''' discontinuous.
For the forcing function as given in (16), the results of the calculations indicated no absolute barrier to particles, with initially low velocity in the stochastic region, diffusing to high velocity; for the function in (17) there existed an absolute barrier to diffusion as predicted by (14). Thus, we not only resolve the question posed by Pustylnikov, but also arrive at the interesting result that, at least for the particular problem treated here, only two continuous derivatives of F are necessary for the existence of an isolating KAM surface.

III DIFFUSION IN THE STOCHASTIC REGION

We consider the Ulam version of Fermi acceleration with KAM surfaces bounding the stochastic region from above. In regions I and II, in those portions of the phase plane which are accessible to a stochastic trajectory, the trajectory ergodicly covers the phase plane. This implies that after long times, the probability density is uniform over the phase plane (see, for example, Arnold and Avez [15]). Furthermore, in the low velocity region I, for which no significant size adiabatic islands exist, an integration over phases results in a uniform probability density $\bar{f}$ versus the canonically conjugate action. For the sawtooth wall velocity Lieberman and Lichtenberg [6] computed the density $\bar{f}(u)$ both for the simplified mapping, for which momentum is imparted without physical wall movement, and for the exact mapping, as given by Zaslavskii and Chirikov [4]. Although the sawtooth wall velocity does not strictly satisfy the boundedness condition for ergodicity, the diffusion into the adiabatic region III is sufficiently slow that approximate agreement is expected. The results of the computation, however, while giving the expected result for the simplified equations, gave an $\bar{f}(u) \propto u$ for the exact equations. The reason for this apparent contradiction is that, for the exact problem, as first pointed out by Brahic [5], the variables u_n and ϕ_n are not canonical conjugates. As we shall show below, if the phase is defined as that at the time of collision with the fixed wall, the variable conjugate to the phase is the energy $E = u^2$. If $\bar{f}(E) = f_o$ then

$$f(u) = f(E) \frac{dE}{du} \propto u \tag{18}$$

which is the result found numerically. These ideas have been developed by Izrailev and Zhadanova [16] in order to explain the numerical results. They also performed numerical calculations in support of their discussion, finding $f(u^2) = \text{constant}$.

To see how the canonical variables are formed, we write the difference equations in terms of collisions with the fixed, rather than the moving, wall. Defining $w_n = v_n/2\omega a$ to be the normalized velocity and ψ_n to be the phase of the moving wall at the n^{th} collision of the particle with the fixed wall, then we have, in implicit form, analogous to Eqs. (1) and (2), the exact equations of motion

$$w_{n+1} = w_n - F'(\phi_c) \tag{19}$$

$$\psi_{n+1} = \phi_c + [\pi M + \frac{1}{2} F(\phi_c)]/w_{n+1} \tag{20}$$

$$\phi_c = \psi_n + [\pi M + \frac{1}{2} F(\phi_c)]/w_n \tag{21}$$

where ϕ_c is the phase at collision with the moving wall, after the n^{th} collision with the fixed wall, and $M = \ell/2\pi a$. In this form it is easy to see that, measuring the distance from the fixed wall as x, conjugate to v, then the phase ψ is a timelike variable conjugate to E. That is, in the extended phase space $(v,x,E,-t)$ the choice of a surface of section at $x = 0$ gives an area preserving motion for the remaining pair $(E,-t)$. This can be confirmed by direct computation of the Jacobian from (19)-(21), with $E = w^2$,

$$\frac{\partial(E_{n+1},\psi_{n+1})}{\partial(E_n,\psi_n)} = 1 . \tag{22}$$

This result is in contrast to the simplified form of the problem in which the physical wall motion is neglected by dropping F in (20) and (21). These equations are then equivalent to (1) and (2), with $\omega\tau = 2\pi M/u_{n+1}$, for which the phase ϕ at collision with the moving wall is a position-like variable and therefore conjugate to u. This can be directly confirmed by calculating

$$\frac{\partial(w_{n+1},\psi_{n+1})}{\partial(w_n,\psi_n)} = \frac{\partial(u_{n+1},\phi_{n+1})}{\partial(u_n,\phi_n)} = 1 . \tag{23}$$

We now calculate $\bar{f}(u)$, directly, for the simplified and exact problems, for velocities sufficiently low that a random phase assumption is a good approximation.

As shown in Lieberman and Lichtenberg [6] the evolution of the velocity distribution $f(u,n)$ for the simplified Ulam mapping can be written in terms of a Fokker-Planck equation

$$\frac{\partial f}{\partial \tau} = -\frac{\partial}{\partial u}(Bf) + \frac{1}{2}\frac{\partial^2}{\partial u^2}(Df) \tag{24}$$

where τ is measured in units of bounces and

$$B(u) = \left(\frac{1}{n}\right)\int \Delta u \; P \; d(\Delta u) \tag{25}$$

$$D(u) = \left(\frac{1}{n}\right)\int (\Delta u)^2 \; P \; d(\Delta u) \tag{26}$$

and P is the probability of a particle being at u if it were at $u - \Delta u$, n collisions earlier. Assuming for $n = 1$ that no phase correlations exist, i.e., the phase ϕ_n is uniformly distributed over 2π, one

obtains

$$B = 0 \tag{27}$$

$$D = \frac{1}{2\pi} \int_{-\pi}^{\pi} F'^2(\phi)\, d\phi \ . \tag{28}$$

For a sawtooth wall velocity $F' = \phi/(2\pi)$, and one obtains $D = 1/12$. In the steady state, assuming perfectly reflecting barriers at $u = 0$ and $u = u_s$, one obtains a uniform distribution in velocity $\bar{f}(u) = f_o$.

A similar calculation can be made for the exact Ulam mapping with a sawtooth wall velocity. However, the non-uniform phase distribution at the moving wall must be taken into account. Izrailev and Zhdanov [16] showed that this could be done explicitly be relating the uniform phase at the fixed wall to the nonuniform phase at the moving wall, obtaining the Fokker-Planck coefficients. We here generalize their result to obtain the steady-state distribution, for the exact equations, with arbitrary wall velocity, but do so directly in terms of the canonical variables (E,ψ) . We let $g(E,n)$ be the energy distribution and write the Fokker-Planck equation

$$\frac{\partial g}{\partial n} = -\frac{\partial}{\partial E}(\bar{B}\, g) + \frac{1}{2}\frac{\partial^2}{\partial E^2}(\bar{D} g) \tag{29}$$

which form holds for any canonical variables with

$$\bar{B}(E) = \frac{1}{n}\int \Delta E\ P\ d(\Delta E) \tag{30}$$

$$\bar{D}(E) = \frac{1}{n}\int (\Delta E)^2\ P\ d(\Delta E) \ . \tag{31}$$

From (19) and the definition of E

$$\Delta E = - 2E^{\frac{1}{2}} F' + F'^2 . \tag{32}$$

Then making the random phase assumption for the canonical phase ψ ,

$$\bar{B} = \frac{1}{2\pi} \int_{-\pi}^{\pi} \Delta E \, d\psi . \tag{33}$$

From (21)

$$d\phi_c = d\psi + \frac{1}{2} E^{-\frac{1}{2}} F' \, d\phi_c \tag{34}$$

which gives, since F' is an odd function of ϕ_c ,

$$\bar{B} = \frac{1}{2\pi} \int_{-\pi}^{\pi} 2 F'^2 \, d\phi_c . \tag{35}$$

A similar calculation gives

$$\bar{D} = \frac{1}{2\pi} \int_{-\pi}^{\pi} (4 E F'^2 + 3F'^4) \, d\phi_c . \tag{36}$$

For a sawtooth wall velocity $F' = \phi_c/2\pi$, one finds $\bar{B} = 1/6$ and, $\bar{D} = E/3+3/80$. In the steady state with perfectly reflecting barriers, and neglecting the factor 3/80 in $\bar{D}$, one then finds a uniform distribution in energy $g(E) = g_o$. Since from (18) $f = 2ug$, we find the velocity distribution varies linearly with the velocity u . These results are in agreement with the results of numerical simulations in Lieberman and Lichtenberg ([6], Fig. 12), and Izrailev and Zhadanova ([16], Fig. 3). The first of these figures is reproduced here in Fig. 2, showing the velocity distribution

of the simplified (solid line) and exact (dashed line) Ulam mapping, with a sawtooth wall velocity. The deviations below the stochastic velocity limit, $u_s = M^{\frac{1}{2}}/2 \approx 16$ ($M = 2\omega^2 a\ell = 1000$ in this example), for which all fixed points are unstable, are due to inadequate time for a quasi-steady state to be achieved and to the flux leakage at high velocities. For $u > u_s$ adiabatic islands become increasingly important.

If (19) is transformed into the form of (24), then, from the energy coefficients $\bar{D}$ and $\bar{B}$, we obtain, for the exact Ulam mapping, the velocity coefficients

$$D = \bar{D}/(4E) \tag{37}$$

$$B = (\bar{B} - D)/(2E^{\frac{1}{2}}) \quad . \tag{38}$$

For the sawtooth wall velocity $B = (24u)^{-1}$ and $D = 1/12$, as obtained by Izrailev and Zhadanova [16].

IV. FIXED POINTS AND LINEAR STABILITY

As we have discussed previously in Lieberman and Lichtenberg [6] if we write Eqs. (1) and (2) in matrix form as

$$(u_{n+1}, \phi_{n+1}) = M(u_n, \phi_n) \tag{39}$$

then the periodic points for a k-iterated mapping occur for

$$(u_n, \phi_n) = M^k(u_n, \phi_n) \qquad \phi_n \bmod 2\pi \quad . \tag{40}$$

In the neighborhood of a given fixed point the motion stability can be determined from the tangent (i.e., linearized) mapping

$$(\Delta u_{n+1}, \Delta\phi_{n+1}) = L \cdot (\Delta u_n, \Delta\phi_n) \tag{41}$$

where L is the ordered product of the Jacobian matrices of M. Most of the interesting properties of the mappings have been found from examining the fixed points of a single iteration, $k = 1$.

The simplified Ulam mapping of a particle bouncing between the fixed and oscillating wall, the simplified Pustylnikov mapping of a particle returning to a sinusoidally oscillating wall under gravity, and a class of related mappings, can be expressed in terms of a radial twist mapping

$$I_{n+1} = I_n + K \sin \theta_n \tag{42}$$

$$\theta_{n+1} = \theta_n + G(I_{n+1}) \tag{43}$$

where $G = I_{n+1}$ gives the standard and simplified-Pustylnikov mappings, and $G = 1/I_{n+1}$ gives the simplified Ulam mapping. Generally θ is modulo 2π, but I is not. However, for the standard mapping, (43) implies that I is also modulo 2π, which profoundly effects the fixed points. For $k = 1$, in the general case, substituting (40) in (42) and (43) we have

$$K \sin \theta_o = 0 \tag{44}$$

$$G(I_o) = 2\pi m, \quad m \text{ integer} . \tag{45}$$

For the standard mapping

$$K \sin \theta_o = 2\pi\ell \tag{46}$$

$$G(I_o) = I_o = 2\pi m \quad . \tag{47}$$

The interesting consequence of this difference appears when we examine the stability in the neighborhood of a fixed point. Expanding about fixed point I_o , θ_o we obtain the tangent mapping

$$\begin{bmatrix} \Delta I_{n+1} \\ \Delta\theta_{n+1} \end{bmatrix} = \begin{bmatrix} 1 & K\cos\theta_o \\ G'_o & 1+G'_oK\cos\theta_o \end{bmatrix} \begin{bmatrix} \Delta I_n \\ \Delta\theta_n \end{bmatrix} \tag{48}$$

where $G'_o = \left.\frac{\partial G}{\partial I}\right|_{I=I_o}$. The eigenvalues are given by

$$\begin{vmatrix} 1-\lambda & K\cos\theta_o \\ G'_o & 1+G'_o\cos\theta_o-\lambda \end{vmatrix} = 0 \quad . \tag{49}$$

The motion is stable for the roots λ_1 , λ_2 complex conjugates, satisfied for the discriminant less than zero, i.e.,

$$-4 < G'_oK\cos\theta_o < 0 \quad . \tag{50}$$

For the general case, satisfying (44) $\cos\theta_o = \pm 1$ and K is bounded for stable solutions. In particular for the simplified Ulam mapping, $K < 4I_o^2$ for stability. Since, from the fixed point condition (45), the maximum value of I_o is $1/2\pi$, all first order fixed points are unstable for $K > 1/\pi^2$. In contrast, for the standard mapping, condition (46) allows for finite $\sin\theta_o$ with finite ℓ , and therefore windows of

successively higher values of K exist as ℓ increases ($\cos\theta_o$ decreases). These accelerator modes, so called because the stability regions surround fixed points for which I is monotonically increasing, have been studied in detail by Chirikov [9]. The existence of accelerator modes has also been pointed out by Pustylnikov for his model of Fermi acceleration which is globally approximated by the standard mapping. However, it is clearly inappropriate to discuss accelerator modes for mappings which only locally approximate the standard mapping.

For $k=2$ fixed points the situation changes, and stability may be possible for $K\to\infty$ at fixed action. For the simplified Ulam mapping Lieberman and Lichtenberg [6] showed that $k=2$ primary fixed points, that is, fixed points that exist to zero nonlinearity ($K=0$), were unstable at all values of the action for which $k=1$ fixed points were unstable. They postulated without proof that a value of the action exists below which all fixed points are unstable. In contrast, for the standard mapping, Chirikov [9] showed that windows of stability existed for arbitrary K . We now show that these two contrasting results each belong to distinct classes of mappings.

Period two fixed points with values I_1 , θ_1 , I_2 , θ_2 formed by two iterations of the mapping (42) and (43) can be written in a form which makes explicit the 2π periodicity of θ

$$I_2 = I_1 + K\sin\theta_1 \qquad I_1 = I_2 + K\sin\theta_2 \tag{51}$$

$$\theta_2 = \theta_1 + G(I_2) - 2\pi m \qquad \theta_1 = \theta_2 + G(I_1) - 2\pi n \tag{52}$$

with m and n chosen to keep θ_1 and θ_2 in the range $0-2\pi$. The mapping satisfies the conditions

$$\sin\theta_1 + \sin\theta_2 = 0 \tag{53}$$

$$G(I_1) + G(I_2) = 2\pi(n+m) \quad . \tag{54}$$

Equation (53) implies either:

$$\text{Case (a)} \qquad \theta_1 + \theta_2 = 0 \tag{55}$$

$$\text{Case (b)} \qquad \theta_1 - \theta_2 = \pm\pi \quad . \tag{56}$$

The stability is investigated from the eigenvalues of the tangent mapping

$$\begin{bmatrix} 1 & K\cos\theta_2 \\ G_2' & 1 + G_2'K\cos\theta_2 \end{bmatrix} \begin{bmatrix} 1 & K\cos\theta_1 \\ G_1' & 1 + G_1'K\cos\theta_1 \end{bmatrix} = \lambda \begin{bmatrix} 1 & 0 \\ 0 & 1 \end{bmatrix} \tag{57}$$

which, for complex conjugate λ , requires

$$-4 < (G_1'+G_2')(K\cos\theta_1 + K\cos\theta_2) + G_1'G_2'K^2\cos\theta_1\cos\theta_2 < 0 \; . \tag{58}$$

We first examine Case (b), the algebraically simpler case but with results typical of both of them. Without loss of generality we choose the positive sign in (56) such that $K\cos\theta_1 + K\cos\theta_2 = 0$. Substituting this in (58) the condition for stable fixed points reduces to

$$0 < G_1'G_2'K^2\cos^2\theta_1 < 4 \; . \tag{59}$$

Writing $K\cos^2\theta_1 = K^2 - K^2\sin^2\theta_1$, then from (44) we have

$$K^2\cos^2\theta_1 = K^2 - (I_2 - I_1)^2 \tag{60}$$

which substituted in (59) gives

$$(I_2 - I_1)^2 < K^2 < (I_2 - I_1)^2 + \frac{4}{G_1'G_2'} \; . \tag{61}$$

Combining (52) with (56) we have

$$G(I_2) = (2m - 1)\pi \tag{62}$$

$$G(I_1) = (2n + 1)\pi \ . \tag{63}$$

Solving (62) and (63) for I_2 and I_1, respectively, and substituting into (61), we obtain the stability windows for K. In particular, for the standard mapping with $G(I) = I$ and $G_1' = G_2' = 1$ we obtain Chirikov's result for the stability windows,

$$(2\ell\pi)^2 < K^2 < (2\ell\pi)^2 + 4 \tag{64}$$

where $\ell = m-n-1$ takes on all integer values. Thus, windows of stability exist for arbitrarily large K.

In contrast, if we choose $G(I) = I^{-1}$, we have

$$(I_2 - I_1)^2 = \left(\frac{1}{(2m - 1)\pi} - \frac{1}{(2n + 1)\pi} \right)^2 \tag{65}$$

and

$$G_1'G_2' = (2m - 1)^2(2n + 1)^2 \pi^4 \ . \tag{66}$$

Using (65) and (66) it is then easily seen that the right hand side of (61) has a maximum value of $4/\pi^2 + 4/\pi^4$ for $m = 0$ and $n = 0$, which when substituted into the right hand side of (61) gives the stability condition

$$K < \left(\frac{4}{\pi^2} + \frac{4}{\pi^4} \right)^{\frac{1}{2}} \ . \tag{67}$$

The simplified problem of the particle bouncing between fixed and oscillating walls is described by $G(I) = I^{-1}$; hence, Equations (65) and (66) apply. However, exclusion of negative velocities, and hence negative I's , from the physical problem, precludes the possibility of having $m = n = 0$. Then the right hand side of Eq. (61) takes on its maximum value of $4/\pi^4$ at $m = 1$, $n = 0$, so that we have the stability condition

$$K < 2/\pi^2 . \qquad (68)$$

For this case, $I_1 = I_2$, which is also the condition that the fixed points exist and are stable down to $K = 0$. Although the K in (68) is larger than that found forthe stability limit of the $k = 1$ fixed point, the result is in agreement with Lieberman and Lichtenberg [6], who stated that fixed points at normalized velocity $u_o = I_o/K$ become unstable at a higher value of u_o for $k = 2$ fixed points than for $k = 1$ fixed points at a fixed value of $M = (2\pi K)^{-1}$. The stability limits are, in fact, identical but the normalization makes them appear in reverse order.

More generally, if we set $G(I) = I^{\alpha}$, there is an infinite set of windows, to arbitrarily high K , for $\alpha > 0$ and only one window for $\alpha < 0$. These are the two generically different cases for $k = 2$ type (b) fixed points. As noted by Chirikov, for the standard mapping, the size of the stable islands rapidly becomes small for large K . Therefore, the islands have little influence on the macroscopic diffusion properties of the phase space.

We now present the results for Case (a). From (55) we have

$$K\cos\theta_1 = K\cos\theta_2 = K\cos\theta \tag{69}$$

and the stability condition (58) becomes

$$-4 < 2(G_1' + G_2')\, K\cos\theta + G_1'G_2'(K\cos\theta)^2 < 0 . \tag{70}$$

If $G_1' = G_2' = G'$, which includes the standard mapping, (70) reduces to

$$-4 < 4G'K\cos\theta + (G'K\cos\theta)^2 < 0 . \tag{71}$$

Adding 4 to each inequality and taking the square root we find that (71) gives the same stability condition as found for the first order islands in (50), a result found for the standard mapping by Chirikov [9].

The more general case of $G_1' \neq G_2'$ leads to a variety of stability windows. We restrict our detailed analysis to the simplified Ulam problem with $G = I^{-1}$. For this case, evaluating (70) at the two limits, we obtain the following windows for stability

$$-2(I_1^2 + I_2^2) < -K\cos\theta < -2I_2^2 \tag{72}$$

and

$$-2I_1^2 < -K\cos\theta < 0 \tag{73}$$

where $I_2 > I_1$. I_1 and I_2 are found from (52), together with (55), giving

$$I_2 = \frac{1}{2m\pi - 2\theta_1} \tag{74}$$

$$I_1 = \frac{1}{2m\pi + 2\theta_1} \quad . \tag{75}$$

Since (72) and (73) depend on phase as well as K, we use the fixed point relations to eliminate K, solve for θ and then K. Substituting (74) and (75) in (51) we obtain

$$K\sin\theta_1 = \frac{1}{2m\pi - 2\theta_1} - \frac{1}{2n\pi + 2\theta_1} \quad . \tag{76}$$

Dividing the inequalities in (72) and (73) by (76), we eliminate K. As we shall see, in a particular example given below, θ increases and K increases with decreasing magnitude of $K\cos\theta$, such that we examine $K\cos\theta$ at the limit of zero to obtain the maximum stable K at $\cos\theta_1 = 0$ or $\theta_1 = \pi/2$. Substituting this value of θ_1 into (76) we obtain for K

$$K = \frac{1}{2(m - 1/2)\pi} - \frac{1}{2(n + 1/2)\pi} \tag{77}$$

which has a maximum value for $m = 1$, $n = -1$ of

$$K = \frac{2}{\pi} \quad . \tag{78}$$

Comparing (78) with (67) we find for type (a) fixed points that the maximum value of K is limited to a slightly lower value than that found for type (b) fixed points. We shall discuss these interrelations for a particular example. First we summarize the more general results.

Still restricting ourselves to $G(I) = I^{\alpha}$ we find that, for $\alpha > 0$, as in Case (b), there is an infinite set of windows of stability with increasing K , including arbitrarily large values of K . For most negative values of α there are only stable fixed points at small values of K . This includes the case $\alpha = -1$, as we have just shown. Exceptional cases arise, however, for rational α's of the form $\alpha =$ odd integer/even integer with α slightly exceeding 1; for these particular α's there is a finite range of large K for which stable 2^{nd} iteration fixed points exist.

If we consider the simplified version of the Ulam mapping, given by (1) and (2), with the mapping period given by (3), then we have a phase advance parameter (as used in Lieberman and Lichtenberg, 1972)

$$\frac{2\pi M}{u} = \frac{2\omega^2 a\ell}{u} \tag{79}$$

which, when compared with the general twist mapping of (42) and (43), relates M and K by

$$K = \frac{1}{2\pi M} \quad . \tag{80}$$

For a physical problem M is a constant and the phase space is examined for islands (stable KAM curves) as a function of the action. We have taken this point of view in Sec. II.

However, the evolution of a particular fixed point is continuous with M (or K), rather than action. We therefore choose a particular $2\pi m$ in (45) at a $k = 1$ fixed point. We then vary the value of K to determine the evolution of both $k = 1$ and $k = 2$ fixed points. Consider

the particular example of $m=3$. From (45) $I_o = 1/2\pi m$ and from (50), the edge of the period 1 stability window occurs at

$$K = 4I_o^2 = \frac{4}{(2\pi m)^2} \quad . \tag{81}$$

From (81), with $m=3$, $K=.01125$ and from (80) the corresponding $M=14.137$. Also, an expansion around the $m=3$ fixed point to obtain the standard mapping, as in (12) and (13) gives the result

$$\bar{K} := K/I_o^2 = 4 \quad . \tag{82}$$

This is the standard form for expressing the loss of stability at the $k=1$ fixed point.

If we now examine the $k=2$ fixed point condition, (76), with $m=n$, and combining terms we obtain

$$K\sin\theta = \frac{4\theta}{(2\pi m)^2 - (2\theta)^2} \quad . \tag{83}$$

The minimum value of K for which (83) has a solution is $K=4/(2\pi m)^2$ (at $\theta=0$), which is identical to the maximum stable K found for the $k=1$ fixed point. For $\theta>0$ we have $K>4/(2\pi m)^2$, and we find from (72) and (50) stable $k=2$ and unstable $k=1$ fixed points. Thus, we have the generic result that the loss of stability of a k'th iterate fixed point occurs at a bifurcation into a stable $2k$ iterate.

To find the other edge of the $k=2$ stable window we equate the right hand inequality in (72), to obtain

$$K\cos\theta = \frac{2}{(2\pi m - 2\theta)^2} \tag{85}$$

which combined with (83) gives

$$\frac{\tan\theta_1}{\theta_1} = \frac{2(\pi m - \theta_1)^2}{(\pi m)^2 - \theta_1^2} \quad . \tag{86}$$

For $m = 3$, $\theta_1 = 1.05$ radian , and, from (85),

$$K = \frac{1}{2\cos(1.05)\left[(\pi m)^2 - (1.05)^2\right]} \quad , \tag{87}$$

giving roughly a 20 percent increase in K to $K = 0.0137$ and corresponding $M = 11.6$. Beyond this value of K we expect a second bifurcation to take place producing $k = 4$ stable fixed points.

With increasing K (decreasing M) but holding m constant a second window of stability appears. Using (73) with with (75) we find the window occurs (in θ) between

$$1.17 < \theta < \frac{\pi}{2} \quad , \tag{88}$$

and (in K) between

$$\frac{1.27}{(\pi m)^2 - (1.17)^2} < K < \frac{\pi/2}{(\pi m)^2 - (\pi/2)^2} \quad .$$

For $m = 3$ this gives K between 0.0145 and 0.0182 , with the corresponding M between 10.97 and 8.75 . We now observe a very interesting phenomenon. As $\theta = \pi/2$, the type (a) $m = m_o$ fixed points become degenerate with

two pairs of type (b) fixed points each with $m = n = m_o$ we have already found the limit for stability of type (b) fixed points in (61). Considering unequal values of I_1 and I_2 (not primary fixed points) we can obtain I_1 and I_2 identical to the values found for the type (a) fixed points at this limit. In this case for $m = n = 3$, $I_1 = 1/5\pi$ and $I_2 = 1/7\pi$. The type (b) fixed points then have a narrow window of stability in the range (from (61))

$$\left(\frac{1}{5\pi} - \frac{1}{7\pi}\right)^2 < K^2 < \left(\frac{1}{5\pi} - \frac{1}{7\pi}\right)^2 + \frac{4}{5^2 \cdot 7^2 \cdot \pi^4} \quad .$$

The lower limit in K is $K = 0.0182$ corresponding to $M = 8.75$. The upper limit in K is $K = 0.0191$, corresponding to an $M = 8.34$. There are no other stable $k = 2$ fixed points associated with the $k = 1$ $m = 3$ fixed point bifurcation. If we increase K (decrease M) further we reach the value where the $k = 1$ $m = 2$ fixed point becomes unstable at $K = 1/4\pi^2$, $M = 2\pi$, beyond which there is a new set of bifurcations.

The results described above, for the stability windows with $m = 3$ are summarized in the diagram of Fig. 3. A linear scale of K is shown together with the corresponding values M on a reciprocal scale. The positions of a set of illustrative mappings, given in Fig. 4, are also indicated.

We illustrate the above with a set of computer calculations of the mapping, the positions of which are shown in Fig. 3. In Fig. 4a the $k = 1$ $m = 3$ fixed point is shown, together with an associated KAM orbit, for $K = 0.01$, slightly under the value at which the fixed point becomes unstable. Increasing K to $K = 0.0116$ we observe in Fig. 4b the stable type

(a) $k=2$ fixed points which have bifurcated out of the now unstable $k=1$ fixed point. At the bifurcation a stable KAM curve continues to surround the set of two stable $k=2$ fixed points and one unstable $k=1$ fixed point, thus separating the thin stochastic layer in the neighborhood of the separatrix formed by the unstable $k=1$ fixed point from the larger stochastic sea. In Fig. 4c distorted islands, associated with the $k=2$ fixed points are seen for $K=0.0135$ just below (in K) the upper edge of the stable window. The last KAM surface surrounding both fixed points has disappeared so that the orbits near the bifurcated $k=1$ fixed point merge with the stochastic sea. Increasing K to 0.0138, just beyond the stable $k=2$ window we observe in Fig. 4d (on a scale blown up around the lower island) the now unstable $k=2$ 2-point and the bifurcated $k=4$ stable islands. In Fig. 4e (still on an expanded scale), at $K=0.155$, the $k=2$ fixed point has reappeared in the second type (a) stability window; and finally, in Fig. 4f, at $K=0.0184$, the pair of $k=2$ type (a) fixed points has been transformed into two pairs of $k=2$, type (b), $n=m=3$ fixed points, each associated with a different set of initial conditions.

V. CONCLUSIONS

Although no rigorous theory exists to predict the detailed behavior of mappings, such as that given by (1) and (2), the heuristic methods used in treating various forms of the problem by Zaslavskii and Chirikov [4], Lieberman and Lichtenberg [6], and Chirikov [9] quantitatively describe the important features. Various results which appear contradictory can be explained by variations in the forms of the mappings used, and theoretical results are in agreement with numerical computations where compared. The heuristic results are also consistent with all rigorously derived results.

In particular, we have considered the following effects:

(1) If a mapping can be locally approximated by the standard mapping, then the results from the standard mapping can be used to predict the value of action at which KAM surfaces isolate the main connected stochastic region from other parts of the phase space for the mapping being approximated.

(2) The details of the probability distribution within a bounded stochastic portion of the phase space depend on the details of the mapping, but if canonical variables are employed, the ergodic hypothesis appears to be satisfied, when computed over sufficiently long times, leading to a uniform density distribution in phase space.

(3) Fine details of the phase space structure can be markedly different for different mappings, even if they can be locally approximated by the standard mapping. Stability persists around two-iteration fixed points near certain arbitrarily large values of the

stochasticity parameter K for a class of mappings including the standard mapping, while the maximum value of K is strictly limited for another class of mappings including that of a particle confined between a fixed and oscillating wall. For the latter configuration, bifurcations at the stability boundaries are shown both analytically and in a numerical example. The standard mapping does not have these bifurcations because of its particular symmetry properties. Accelerator modes are peculiar to the double periodicity of the standard mapping.

These results indicate that some, but not all, properties of a particular mapping can be deduced from simpler approximations. Locally approximating a mapping by the standard mapping can be useful for determining the existence of isolating KAM surfaces. The standard mapping has, however, special symmetries which endow it with properties that are not generic to wider classes of mappings. Because the mappings considered here have many of the characteristics of two degree of freedom nonlinear Hamiltonian systems, their behavior is useful in qualitatively understanding the more general dynamical problems, but some care must be exercised in relating the fine-scale properties of the various systems.

ACKNOWLEDGMENT

This work was partially supported under ONR Grant N00014-79-C-0674, NSF Grant ENG-7826372, and DOE Contract W-7405-ENG-48.

REFERENCES

[1] E. Fermi, Phys. Rev. 15, 1169 (1949).

[2] S. Ulam, Proc. 4th Berkeley Symp. on Math. Stat. and Prob. 3, 315, Univ. of Calif. Press (1961).

[3] J. M. Hammersley, Proc. 4th Berkeley Symp. on Math. Stat. and Prob. 3, 79, Univ. of Calif. Press (1961).

[4] G. M. Zaskavskii and B. V. Chirikov, Soviet Physics Doklady 9, 989. (1965).

[5] A. Brahic, Astr. and Astrophys. 12, 98 (1971).

[6] M. A. Lieberman, and A. J. Lichtenberg, Phys. Rev. A 5, 1852 (1972).

[7] V. I. Arnold, Russian Math. Surveys 18, 9 (1963).

[8] L. D. Pustylnikov, Trans. Moscow Math. Society 2, 1 (1978).

[9] B. V. Chirikov, Physics Reports 52, 263 (1979).

[10] G. M. Zaslavskii, Statistical Irreversibility in Nonlinear Systems, Novosibirsk, 1968 (in Russian).

[11] J. Moser, Stable and Random Motions in Dynamical Systems, Ann. of Math, 77, Princeton Univ. Press, Princeton, N.J. (1973).

[12] R. H. Cohen, Intrinsic Stochasticity in Plasmas, G. Laval and D. Gresillon, ed., 181 (1979).

[13] J. M. Greene, J. Math. Phys. 20, 1183 (1979).

[14] A. J. Lichtenberg, Intrinsic Stochasticity in Plasmas, G. Laval and D. Gresillon, ed., 13 (1979).

[15] V. I. Arnold and A. Avez, Ergodic Problems of Classical Mechanics, Benjamin, N.Y. (1968).

[16] F. M. Izrailev and T. A. Zhadanova, "On Statistical Fermi Acceleration" Report, Institute of Nuclear Physics, Novosibirsk (1974).

FIGURES CAPTIONS

FIG. 1 (a) Ulam version of Fermi acceleration, in which a particle bounces back and forth between an oscillating wall and a fixed wall separated by a distance ℓ .

(b) Pustylnikov version, in which a particle repeatedly returns to an oscillating wall under the action of a constant gravitational acceleration g .

FIG. 2 Comparison of velocity distribution $\bar{f}(u)$ of the exact equations (dashed line) and the simplified equations (solid line) for the Ulam model with a sawtooth wall velocity ($M = 2\omega^2 a\ell = 1000$).

FIG. 3 Summary of stability windows for period 2 fixed points with $G(I) = I^{-1}$.

FIG. 4 Mappings in the neighborhood of $k=1$ and $k=2$ fixed points with increasing perturbation parameter, indicating the behavior in the various stability windows. Each mapping includes a few initial conditions, depicting both stable and unstable behavior.

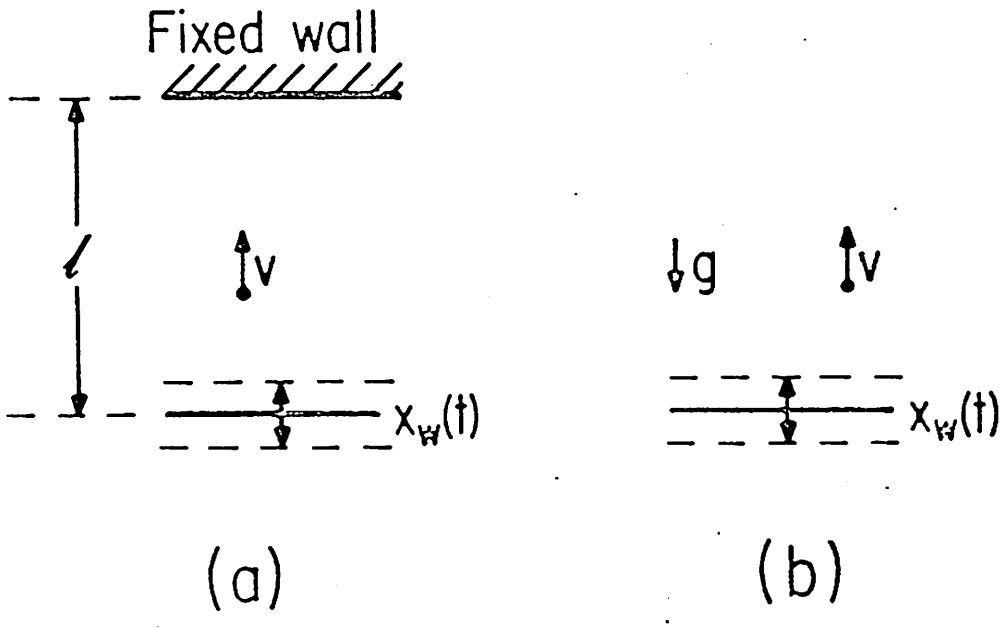

FIGURE 1

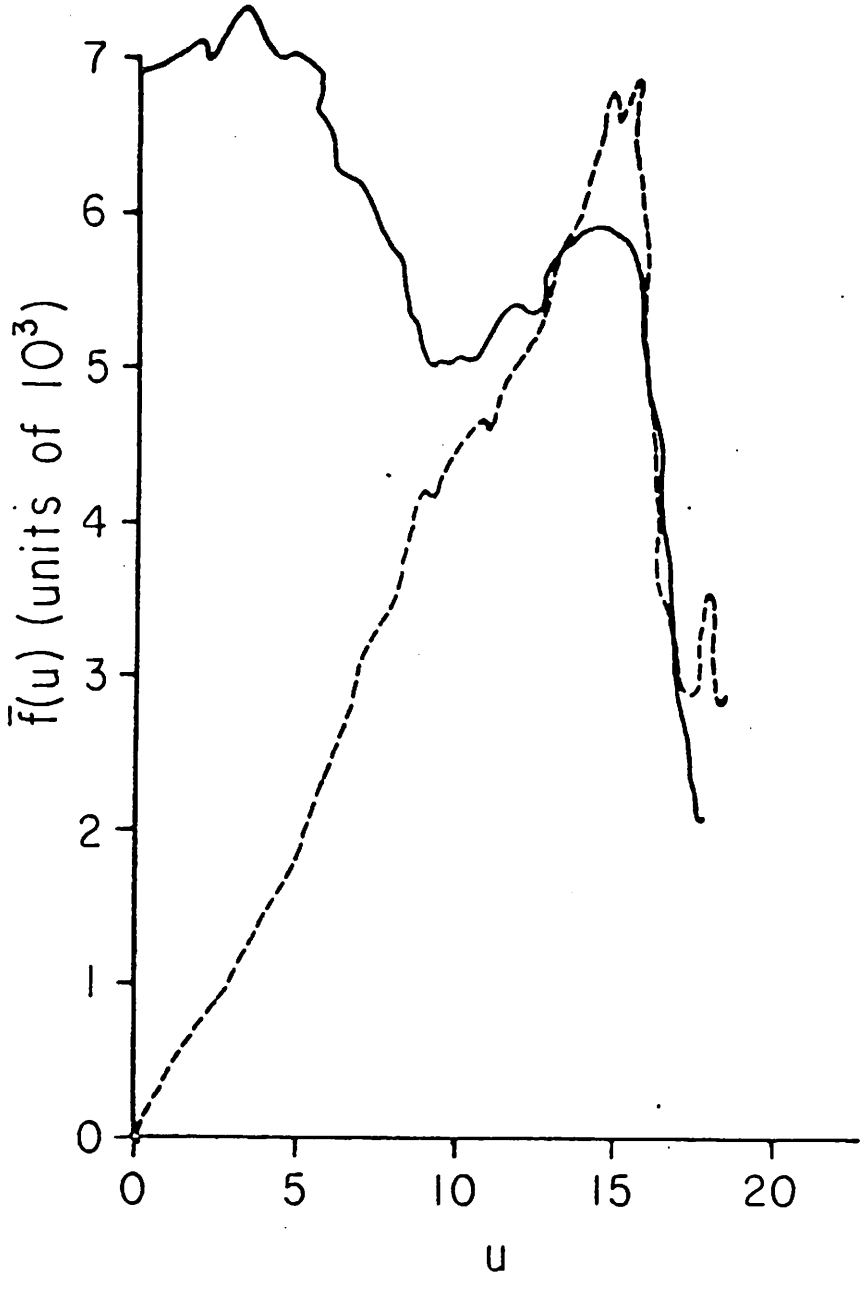

FIGURE 2

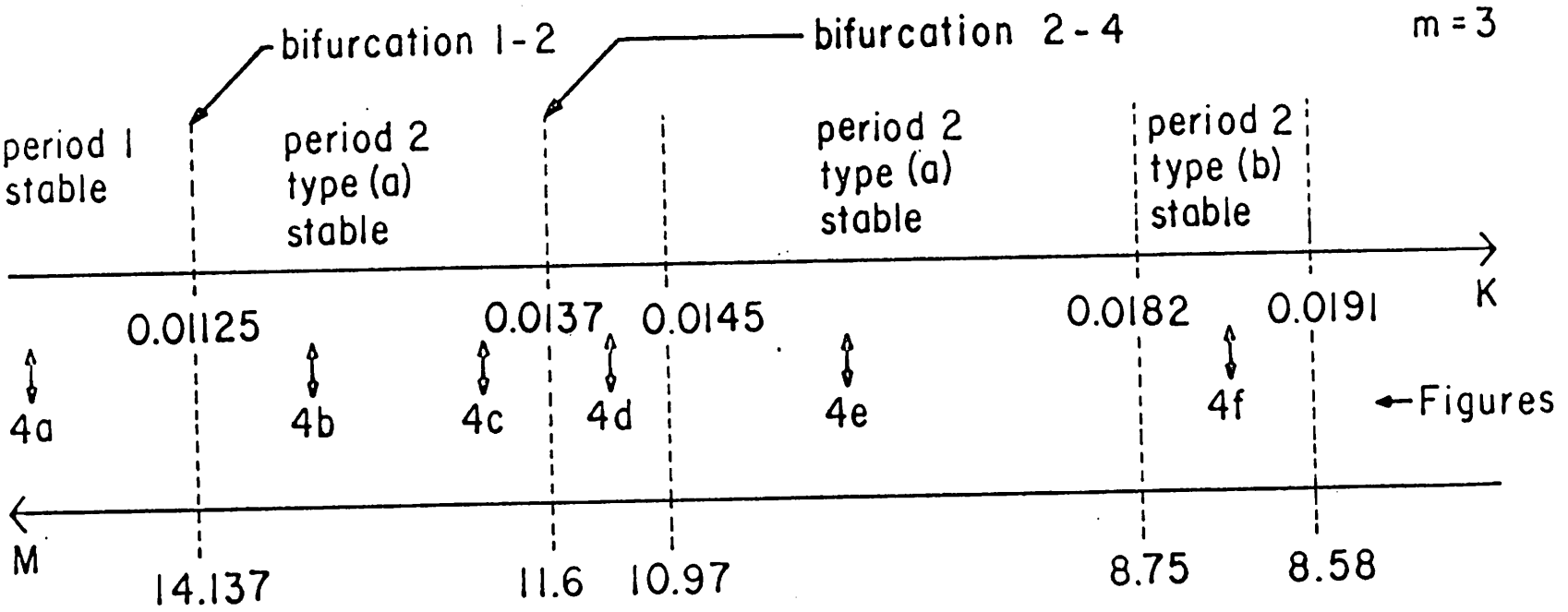
bifurcation 1-2
bifurcation 2-4
m = 3
period 1
stable
period 2
type (a)
stable
period 2
type (a)
stable
period 2
type (b)
stable
K
0.01125
0.0137
0.0145
0.0182
0.0191
4a
4b
4c
4d
4e
4f
Figures
M
14.137
11.6
10.97
8.75
8.58

FIGURE 3

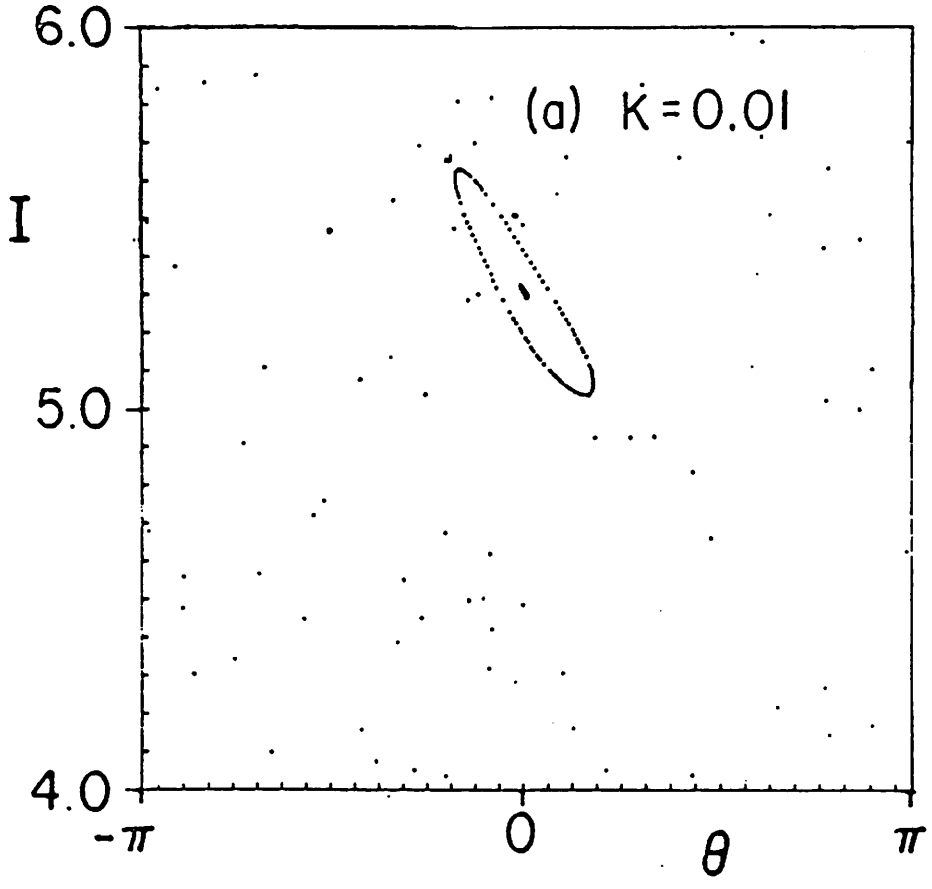

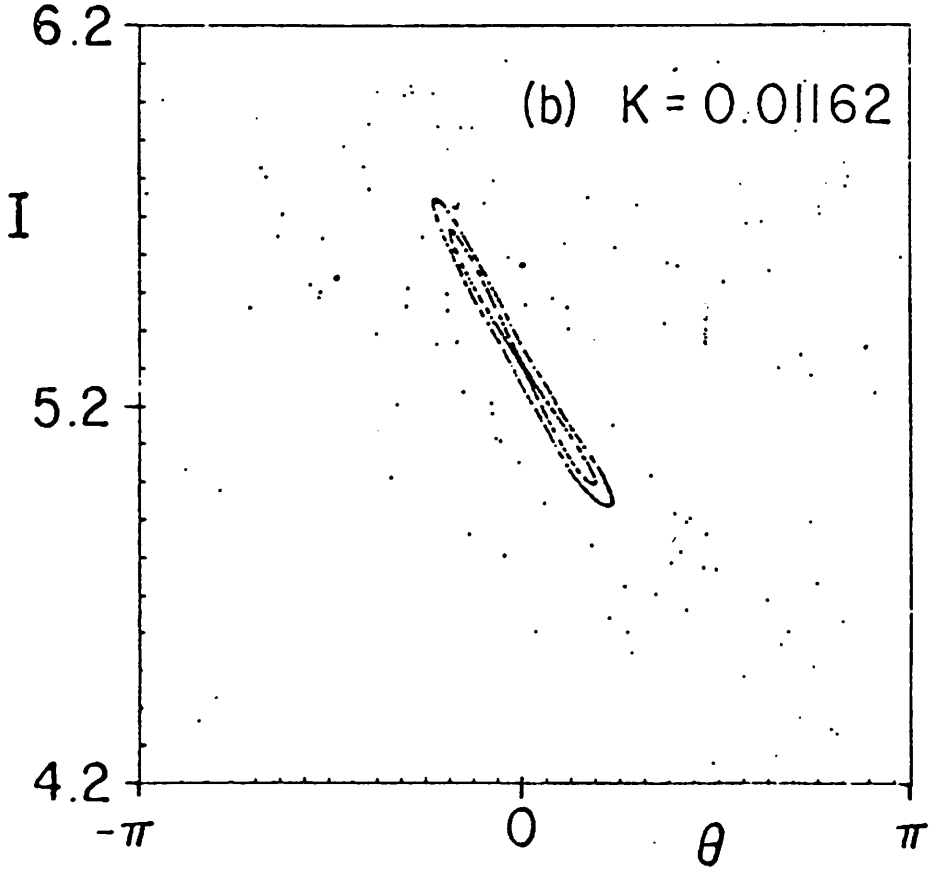

FIGURE 4a & b

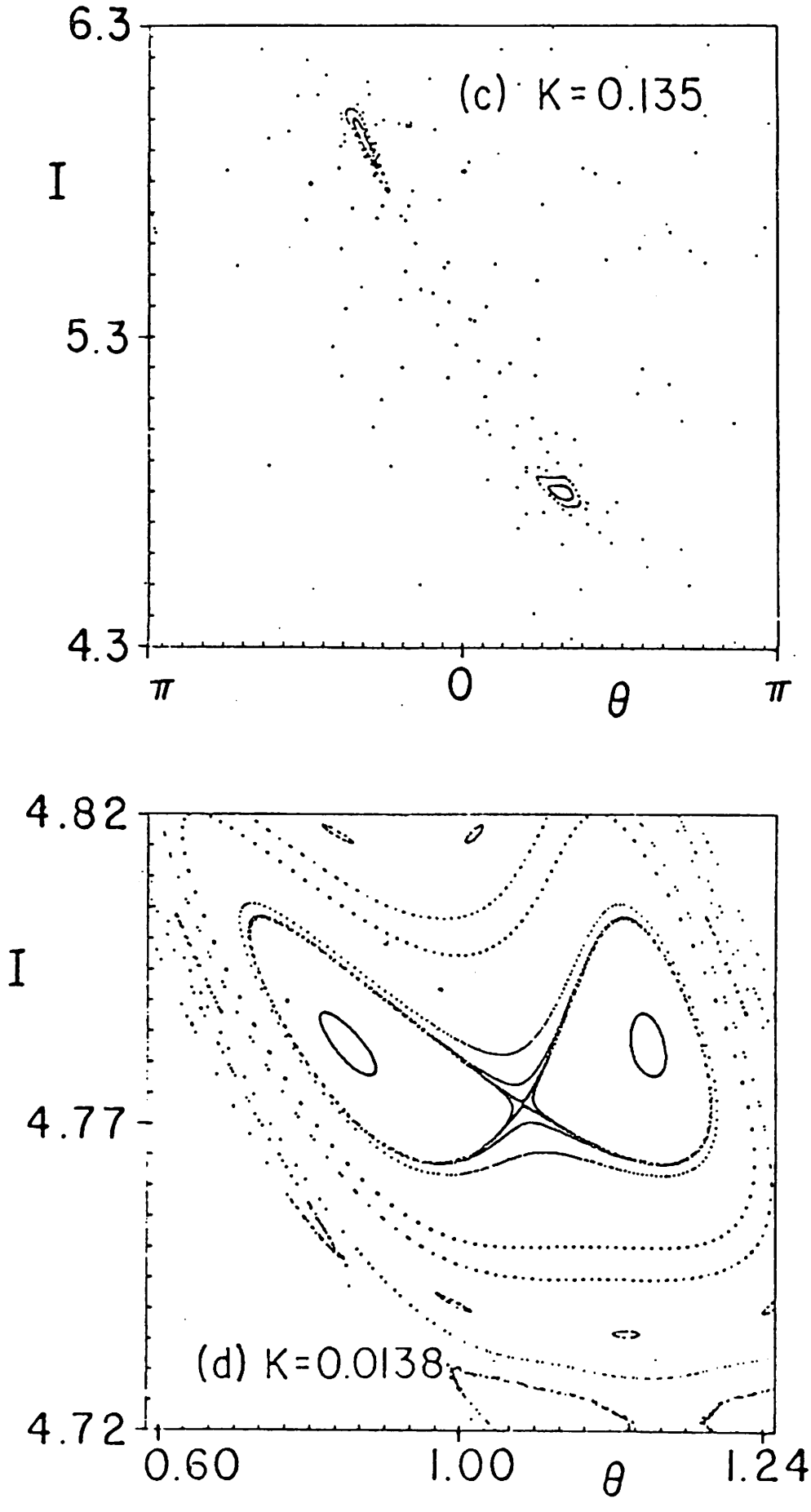

FIGURE 4c & d

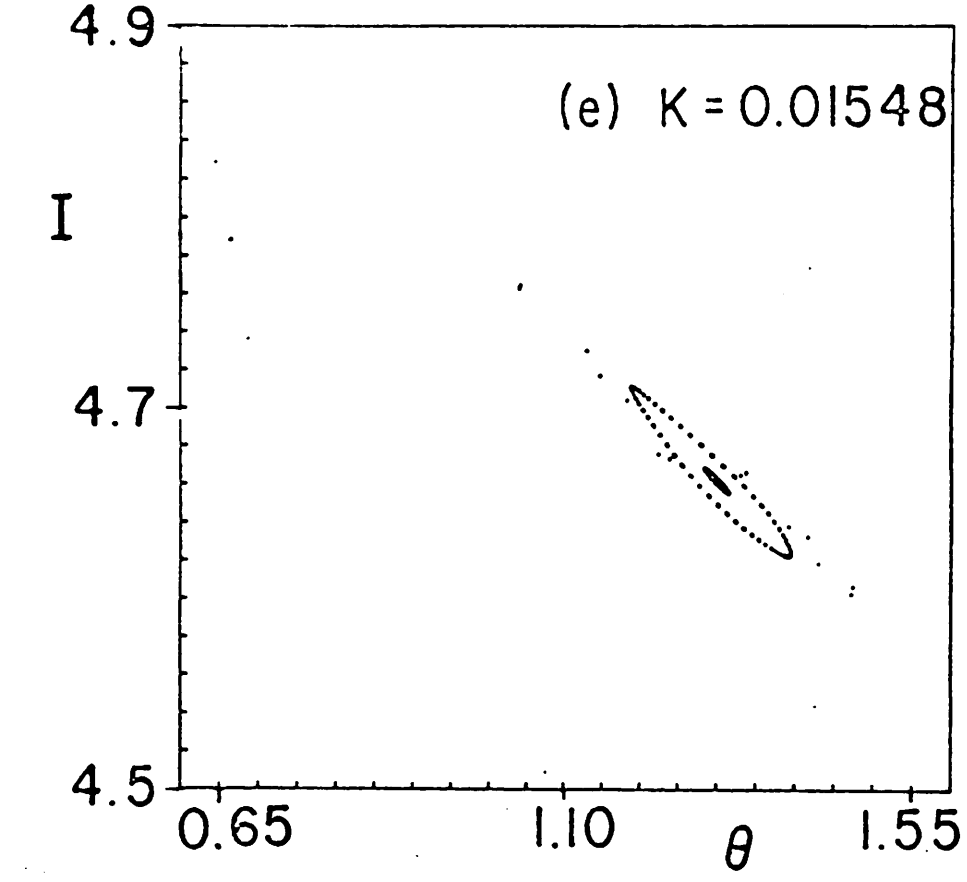
4.9
(e) K = 0.01548
I
4.7
4.5
0.65
1.10
θ
1.55

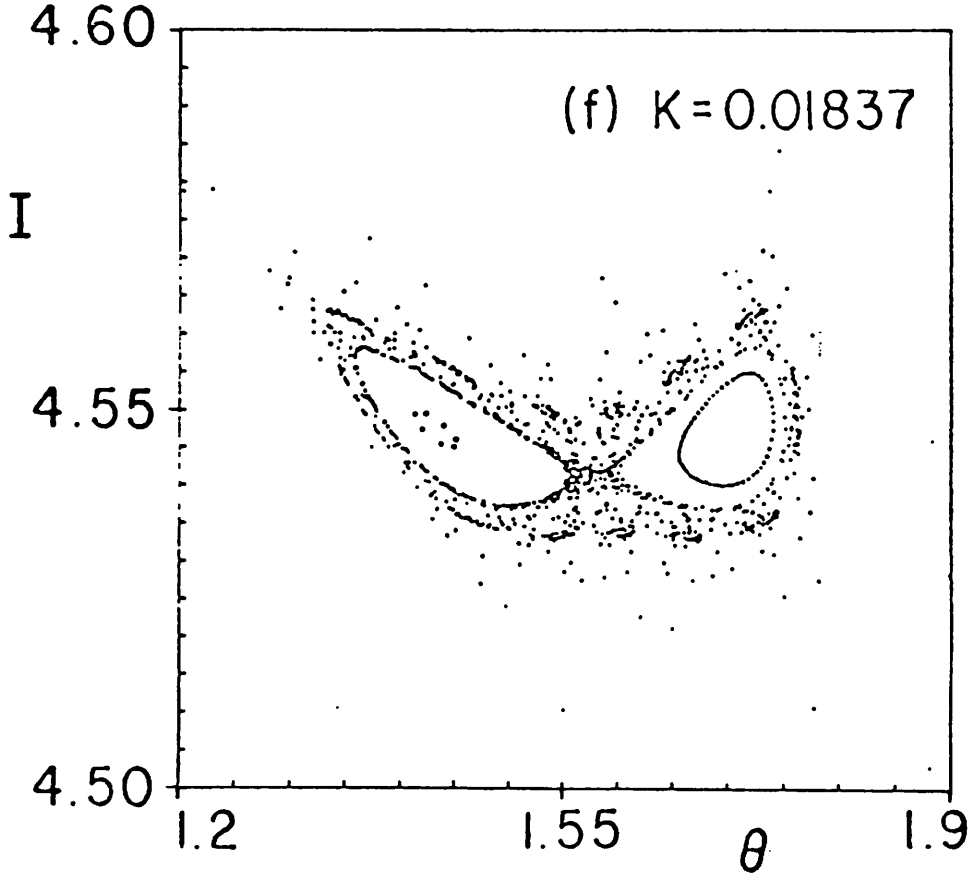
4.60
(f) K = 0.01837
I
4.55
4.50
1.2
1.55
θ
1.9

FIGURE 4e & f